Identification and Chemistry of C_4H_3 and C_4H_5 Isomers in Fuel-Rich Flames

Nils Hansen,*,† Stephen J. Klippenstein,*,†,⊥ Craig A. Taatjes,† James A. Miller,† Juan Wang,‡ Terrill A. Cool,‡ Bin Yang,§ Rui Yang,§ Lixia Wei,§ Chaoqun Huang,§ Jing Wang,§ Fei Qi,*,§ Matthew E. Law,|| and Phillip R. Westmoreland||

Combustion Research Facility, Sandia National Laboratories, Livermore, California 94551, School of Applied and Engineering Physics, Cornell University, Ithaca, New York 14853, National Synchrotron Radiation Laboratory, University of Science and Technology of China, Hefei, Anhui 230026, China, and Department of Chemical Engineering, University of Massachusetts, Amherst, Massachusetts 01003

Received: November 22, 2005; In Final Form: January 6, 2006

Quantitative identification of isomers of hydrocarbon radicals in flames is critical to understanding soot formation. Isomers of C_4H_3 and C_4H_5 in flames fueled by allene, propyne, cyclopentene, or benzene are identified by comparison of the observed photoionization efficiencies with theoretical simulations based on calculated ionization energies and Franck−Condon factors. The experiments combine molecular-beam mass spectrometry (MBMS) with photoionization by tunable vacuum-ultraviolet synchrotron radiation. The theoretical simulations employ the rovibrational properties obtained with B3LYP/6-311++G(d,p) density functional theory and electronic energies obtained from QCISD(T) ab initio calculations extrapolated to the complete basis set limit. For C_4H_3, the comparisons reveal the presence of the resonantly stabilized CH_2CCCH isomer (*i*-C_4H_3). For C_4H_5, contributions from the CH_2CHCCH_2 (*i*-C_4H_5) and some combination of the CH_3CCCH_2 and CH_3-$CHCCH$ isomers are evident. Quantitative concentration estimates for these species are made for allene, cyclopentene, and benzene flames. Because of low Franck−Condon factors, sensitivity to *n*-isomers of both C_4H_3 and C_4H_5 is limited. Adiabatic ionization energies, as obtained from fits of the theoretical predictions to the experimental photoionization efficiency curves, are within the error bars of the QCISD(T) calculations. For *i*-C_4H_3 and *i*-C_4H_5, these fitted adiabatic ionization energies are (8.06 ± 0.05) eV and (7.60 ± 0.05) eV, respectively. The good agreement between the fitted and theoretical ionization thresholds suggests that the corresponding theoretically predicted radical heats of formation (119.1, 76.3, 78.7, and 79.1 kcal/mol at 0 K for *i*-C_4H_3, *i*-C_4H_5, CH_3CCCH_2, and CH_3CHCCH, respectively) are also quite accurate.

1. Introduction

An understanding of the mechanisms of soot formation is a primary focus of current combustion research. Polycyclic aromatic hydrocarbons (PAHs), many of which themselves pose serious risks to human health,[1,2] are widely considered to be precursors to soot. The formation of benzene, as the first aromatic ring, is essential to the PAH growth process and may be a rate-limiting step in the production of larger PAHs.[3−8] The key proposed pathways to the formation of benzene generally involve reactions of unsaturated hydrocarbon radicals, with resonantly stabilized radicals playing a particularly prominent role. There is considerable uncertainty as to the relative importance of various pathways involving different radicals. The recombination of propargyl radicals (C_3H_3) appears to provide the dominant pathway in most flames.[8] However, a number of other pathways may also be of importance. For example, there has been a longstanding debate regarding the possible importance of even-carbon pathways involving the reaction of C_4H_3 and C_4H_5 radicals with acetylene (C_2H_2).[3,4,9−11]

There are often multiple isomeric forms of the hydrocarbon radicals involved in the proposed benzene formation pathways, with these different isomers generally having quite different chemistries. In this paper, we identify isomers of C_4H_3 and C_4H_5 in fuel-rich allene, propyne, cyclopentene, and benzene low-pressure laminar flames. The *n*-isomers of these radicals ($^{\bullet}CH{=}CH{-}C{\equiv}CH$ and $^{\bullet}CH{=}CH{-}CH{=}CH_2$) are not resonantly stabilized and are less stable by about 12 kcal mol^{-1} than the corresponding resonantly stabilized *i*-isomers ($CH_2{=}C^{\bullet}{-}C{\equiv}CH \leftrightarrow CH_2{=}C{=}C{=}^{\bullet}CH$ and $^{\bullet}CH_2{-}CH{=}C{=}CH_2 \leftrightarrow CH_2{=}CH{-}^{\bullet}C{=}CH_2$).[4] On the other hand, additions of the *n*-isomers to acetylene have been thought to have lower-energy barriers than those for the corresponding additions to the *i*-isomers; the former also have simpler paths to cyclic species than the latter.[4,11]

For *n*-C_4H_3, recent calculations[12] have predicted that the concentrations of *n*-C_4H_3 are simply too small for *n*-C_4H_3 + C_2H_2 to yield an effective benzene formation pathway. Also, the addition barrier for *i*-C_4H_3 may not be as large as was predicted in earlier theoretical work,[13] suggesting that the *i*-C_4H_3 + C_2H_2 reaction could be more important than previously thought.[11] For C_4H_5, the situation with regard to the *n*- and *i*-isomers is completely analogous. However, in this case, there are three additional resonantly stabilized isomers: 1-methylallenyl ($CH_3{-}^{\bullet}C{=}C{=}CH_2 \leftrightarrow CH_3{-}C{\equiv}C{-}^{\bullet}CH_2$), CH_3CHCCH ($CH_3{-}^{\bullet}CH{-}C{\equiv}CH \leftrightarrow CH_3{-}CH{=}C{=}^{\bullet}CH$), and *cyclic*-$C_4H_5$ ($-CH_2{-}^{\bullet}CH{-}CH{=}CH- \leftrightarrow -CH_2{-}CH{=}CH{-}^{\bullet}CH-$). All

* Corresponding authors. N.H.: Email nhansen@sandia.gov; tel. 925-294-6272; fax 925-294-2276. S.J.K.: Email sjk@anl.gov; tel. 630-252-3596; fax 630-252-9292. F.Q.: Email fqi@ustc.edu.cn; tel. 0086-551-3602125; fax 0086-551-5141078.

† Sandia National Laboratories.

‡ Cornell University.

§ University of Science and Technology of China.

|| University of Massachusetts.

⊥ Current address: Chemistry Division, Argonne National Laboratory, Argonne, IL, 60439.

10.1021/jp056769l CCC: $33.50
Published on Web 02/17/2006

five could conceivably play a role in the cyclization process and are expected to be readily formed in flames. The 1-methylallenyl is predicted to be more stable than *i*-C_4H_5 by 2.4 kcal mol^{-1}. Reactions of H atoms with C_4H_2, C_4H_3, C_4H_4, and 1,3-butadiene in rich flames are likely to drive the relative concentrations of *n*- and *i*-radicals close to equilibrium.

Historically, species concentration measurements in low-pressure, one-dimensional laminar flames have largely been made with electron-ionization mass spectrometry (EIMS). Unfortunately, the limited energy resolution of the ionizing electrons has precluded the measurement of the isomeric composition of small hydrocarbon radicals with EIMS. The superior energy resolution of photoionization mass spectrometry (PIMS) allows isomer-specific detection of combustion species, and utilization of bright, easily tunable synchrotron radiation makes this approach exceptionally powerful. For example, this method has been used to identify enols as common intermediates in hydrocarbon combustion.[14,15]

In the present work, identification of different isomers of C_4H_3 and C_4H_5 radicals is accomplished by comparing experimental photoionization efficiency (PIE) spectra with simulated curves based on calculated adiabatic ionization energies and Franck−Condon factor analysis. This approach has been shown to yield definitive identification of even previously undetected radical species.[16] In addition, mole fractions can be calculated by use of empirically estimated photoionization cross-sections, which should be accurate to within a factor of 2 or 3, a level sufficient for modeling the relevant chemistry.

In the fuel-rich flames considered in this paper, *i*-C_4H_3 is detected above the ionization energy of (8.06 ± 0.05) eV, which is in excellent agreement with a computed value of 8.02 eV. A comparison of the measured photoionization efficiency for C_4H_5 with the Franck−Condon simulation reveals the presence of the *i*-C_4H_5 isomer as well as the thermodynamically most stable CH_3CCCH_2 isomer and/or the CH_3CHCCH isomer. The adiabatic ionization energies are experimentally determined to be (7.60 ± 0.05) eV for *i*-C_4H_5 and (7.97 ± 0.05) eV for the CH_3CCCH_2 and CH_3CHCCH mixture, which compare well with calculated ionization energies of 7.55 eV (*i*-C_4H_5) and 7.94 eV (CH_3CCCH_2 or CH_3CHCCH). The predicted lower sensitivity to *n*-C_4H_3 and *n*-C_4H_5 isomers limits the present analysis to determining upper bounds on their concentrations.

2. Experimental Section

The present work is carried out in two low-pressure premixed flame experiments, one at the Chemical Dynamics Beamline at the Advanced Light Source (ALS) at the Lawrence Berkeley National Laboratory and one at the National Synchrotron Radiation Laboratory (NSRL) at Hefei, China. The technique of molecular-beam time-of-flight PIMS used in these studies is fully described elsewhere.[17]

Both experiments consist of a low-pressure flame chamber, a differentially pumped flame-sampling system, and a time-of-flight mass spectrometer (TOFMS). Flame gases are sampled through the 0.20-mm orifice of a quartz sampling cone on the flow axis of a flat-flame burner operated at typical pressures of 30 Torr. Translation of the burner toward or away from the quartz sampling cone allows mass spectra to be taken at any desired position within the flame. A skimmer of 2.0-mm aperture placed 23 mm downstream on the axis of the expanded (10^{-4} Torr) jet forms a molecular beam that passes into the differentially pumped (10^{-6} Torr) ionization region, where it is crossed by tunable vacuum ultraviolet light. The resulting photoions are collected and analyzed by using pulsed-extraction time-of-flight mass spectrometry. The machine at the NSRL is equipped with a reflectron time-of-flight mass spectrometer for ion detection; at the ALS, a 1.3-m linear time-of-flight mass spectrometer is employed.

The ALS machine uses tunable undulator radiation, energy-selected by a 3-m off-plane Eagle monochromator. An energy resolution of either 25 or 40 meV fwhm (measured from the observed width of autoionizing resonances in O_2)[18,19] is employed in the present ALS experiments. At the NSRL, synchrotron radiation from an electron storage ring is energy-selected using a 1-m Seya-Namioka monochromator equipped with two gratings (2400 lines/mm and 1200 lines/mm) covering the wavelength range from 30 to 200 nm. The resolving power ($E/\Delta E$) at the NSRL is between 500 and 1000 depending on the monochromator slit width. A LiF window (1.0-mm thickness) is used to eliminate higher-order radiation of the dispersed light at the NSRL, whereas a rare gas filter removes contributions from higher undulator harmonics at the ALS. In both experiments, the photon flux passing through the ionization region is measured with a silicon photodiode calibrated at the National Institute of Standards and Technology (NIST) for quantum efficiency (electron/photon) for photon energies from 7 to 15 eV.

It is no longer in question that fuel structure has a substantial influence on the relative importance of different reactions contributing to the formation of the first aromatic species. In the present experiments, allene, propyne, cyclopentene, and benzene were used as fuels. Fuel-rich allene and propyne flames are of particular interest, as both molecules are potential precursors for C_3H_3 radicals, thus enhancing the importance of the propargyl recombination process.[8] C_5 species, especially cyclopentadienyl, are proposed as important key species during the formation and consumption of aromatic compounds; therefore, cyclopentene flames are of interest because the cyclopentadienyl radical, a possible precursor of benzene and naphthalene,[5,20] is present in large concentrations. Benzene flames are interesting for at least two reasons. Benzene is the simplest aromatic hydrocarbon and is thus the prototype for aromatic combustion. Aromatics make up a substantial fraction of most real fuels. Thus, the oxidation of benzene is of fundamental interest but has not been exhaustively studied, probably in part because of the complexity of C_6 combustion. Furthermore, although the rate-limiting step in PAH and soot formation is believed to be the formation of benzene, most of the molecular weight growth process happens after benzene formation. Thus, by starting with benzene, we can look at the chemistry leading to higher molecular weight species.

In this experiment, the following flame conditions are used:

- allene or propyne/oxygen/40.8% argon flames with a fuel/oxygen equivalence ratio ϕ (fuel/oxygen ratio relative to a stoichiometric mixture) = 1.80 at a pressure of 25.0 Torr and a cold-flow reagent velocity of 48.2 cm/s.
- cyclopentene/oxygen/25% argon flame with an fuel/oxygen equivalence ratio $\phi = 2.00$ at a pressure of 37.6 Torr and a cold-flow reagent velocity of 54.7 cm/s.
- benzene/oxygen/38.5% argon flame with an fuel/oxygen equivalence ratio $\phi = 1.66$ at a pressure of 35.0 Torr and a cold-flow reagent velocity of 29.2 cm/s.

The sampling cone entrance is positioned within the luminous flame zone of each flame at the following distances from the burner face: allene/propyne flame, 4.0 mm; cyclopentene flame, 3.3 mm; benzene flame, 4.5 mm (ALS) and 6.4 mm (NRSL). At the chosen flame positions, both the C_4H_3 and C_4H_5 ion signals at mass-to-charge ratios *m*/*z* of 51 and 53 appear in the

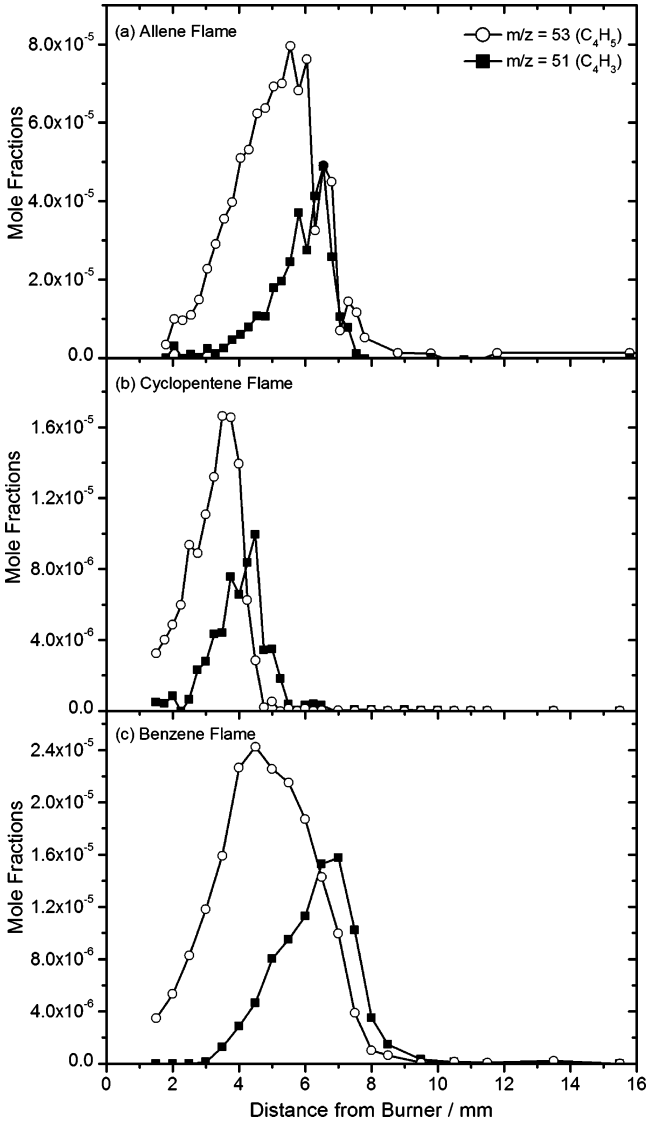

Figure 1. Total C_4H_3 and C_4H_5 mole fractions in a fuel-rich allene/O_2/Ar flame ($\phi = 1.81$), in a fuel-rich cyclopentene/O_2/Ar flame ($\phi = 2.00$), and in a fuel-rich benzene/O_2/Ar flame ($\phi = 1.66$) vs distance from the burner face. The signals were taken at 9.8 eV (allene flame), 10.0 eV (cyclopentene flame), and 9.11 eV (benzene flame). The data points are connected by lines to clarify their positions.

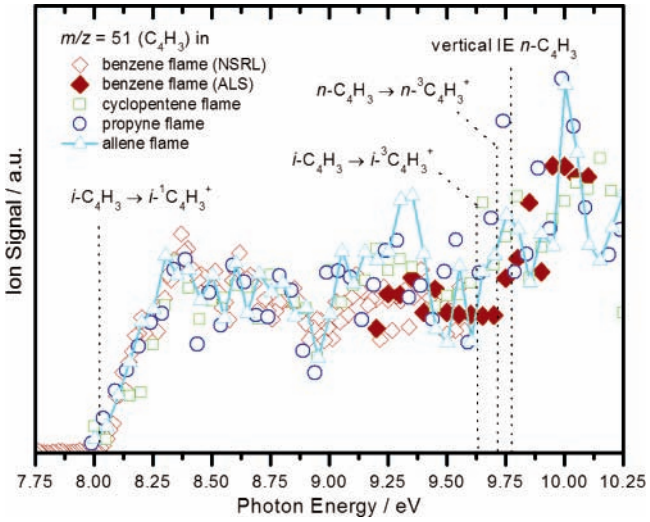

Figure 2. Measured photoionization efficiency curves for $m/z = 51$ (C_4H_3) in fuel-rich allene, propyne, cyclopentene, and benzene flames. Calculated ionization energies of several C_4H_3 isomers are marked. See text for details.

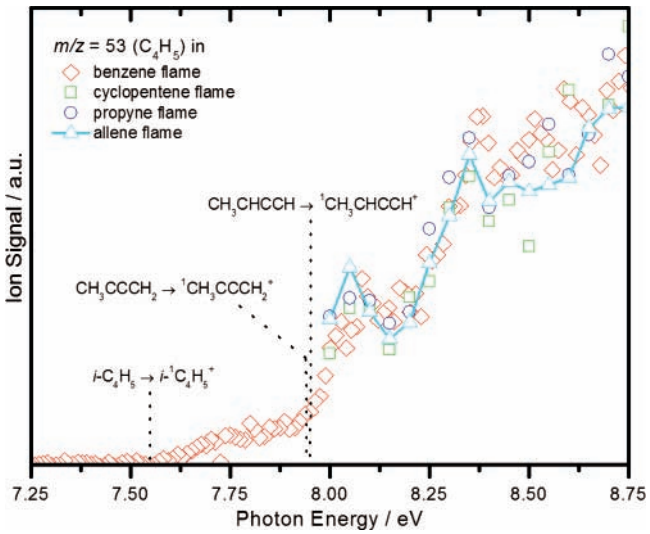

Figure 3. Measured photoionization efficiency curves for $m/z = 53$ (C_4H_5) sampled from fuel-rich allene, propyne, cyclopentene, and benzene flames. Calculated ionization energies of several C_4H_5 isomers are marked. See text for details.

time-of-flight spectrum, as displayed in Figure 1 for the allene, cyclopentene, and benzene flames. The given profiles were taken at 9.80 eV (allene flame), 10.00 eV (cyclopentene flame), and 9.11 eV (benzene flame), and the mole fractions were derived according to a method described earlier by Cool et al.[21] Because of the absence of reference photoionization cross-sections for most radicals, the determination of the absolute concentrations is somewhat uncertain. Nevertheless, we note that there is generally little variation in direct photoionization cross-sections between molecules with similar functional groups, so simple empirical estimates of the expected cross-sections should yield absolute concentrations that are accurate to within about a factor of 2. This level of accuracy is sufficient for many kinetic modeling purposes. Photoionization cross-sections for C_4H_3 and C_4H_5 are estimated to be 10 Mb near 10 eV, based on known absolute cross-sections for propargyl (8.8 Mb), vinyl (12 Mb), and allyl (6.1 Mb).[22,23]

To yield photoionization efficiencies (PIE), the ion signals at a given m/z ratio are obtained by integration of the accumulated ion counts per channel over a 60-ns time interval centered about the mass peak, from which the baseline contribution, obtained from the signal between peaks, is subtracted. This approach permits integration over the entire temporal profile of each mass peak, while avoiding overlapping contributions from adjacent mass peaks. The baseline-corrected ion signals at $m/z = 51$ (C_4H_3) and $m/z = 53$ (C_4H_5) are measured as functions of photon energy and finally are normalized by the photon flux, recorded with the NIST-calibrated photodiode. These flux-normalized ion signals for C_4H_3 and C_4H_5 were corrected for the contributions of ^{13}C and ^2H isotopomers of C_4H_2 and C_4H_4.

Observed PIE spectra are shown in Figures 2 and 3 for the C_4H_3 and C_4H_5 species from each of the flames. Although the number densities of the C_4H_3 and C_4H_5 species differ in each flame, the PIEs of Figures 2 and 3 have been vertically scaled for ease of comparison; it can be seen that the shapes of the PIE curves sampled from different flames are very similar. For C_4H_3, the photoionization efficiency rises abruptly near a well-defined threshold of 8.0 eV and exhibits a second slower increase near 9.6 eV. Poorly resolved structure, suggestive of

strongly broadened vibrational autoionization resonances, is observed above 8.25 eV.

The photoionization efficiency of C_4H_5 shows a small step near 7.6 eV and a larger one close to 8.0 eV. A gradual rise in the photoionization efficiency is observed above 8.2 eV.

3. Computational Methodology

The geometries and harmonic vibrational frequencies of various isomers of the C_4H_3 and C_4H_5 radicals and cations were obtained with density functional theory employing the Becke-3−Lee−Yang−Parr (B3LYP) hybrid functional[24] and the 6-311++G(d,p) basis set.[25] These density functional evaluations, which were performed with *Gaussian 98* and *Gaussian 03* quantum chemical software,[26] employed unrestricted spin wave functions for all open-shell species and spin-restricted wave functions for all singlets.

Higher-level energies, E_{HL}, for these cation and neutral structures are obtained from the basis set extrapolation of quadratic configuration interaction calculations (QCISD(T)) employing Dunning's correlation-consistent triple- and quadruple-ζ basis sets,[27] as described in ref 16. These higher-level evaluations were performed with the MOLPRO[28] quantum chemical software and include the B3LYP/6-311++G(d,p) harmonic zero-point energy corrections. Heats of formation are calculated by considering H_2, CH_4, and CO_2 as reference species.

The simulations of photoionization efficiency spectra based on Franck−Condon factors employ the force-constant matrices, unscaled frequencies, and normal mode displacements calculated at the B3LYP/6-311++G(d,p) level for the neutral and the cation of the isomers considered here. The evaluation of overlap integrals is carried out in the harmonic approximation, accounting for Duschinsky rotation. Multidimensional overlap integrals are evaluated according to recursion relations.[29,30] The calculations are carried out using a program developed by Winter, Zwier, and Lehmann.[31] The resulting Franck−Condon factors, including hot bands arising from thermal population at the assumed temperature, are integrated and convolved with a Gaussian response function corresponding to the measured experimental photon energy resolution of 40 meV (fwhm).

4. Results and Discussion

4.1. Calculated Thermodynamic Properties. *C_4H_3.* There have been numerous theoretical efforts to characterize the isomers of C_4H_3.[12,32−35] In agreement with chemical experience, the acyclic *i*-C_4H_3 and *n*-C_4H_3 radicals are found to be the most stable isomers. In the highest-level calculations, *n*-C_4H_3 is found to be higher in energy by 11.8 kcal mol^{-1} relative to the *i*-C_4H_3 isomer.[35] These calculations, together with the multireference configuration interaction calculations from ref 12, effectively refute the lower isomeric difference predicted by the quantum Monte Carlo calculations of ref 36. Calculated heats of formation (0 K) of various neutral isomers of C_4H_3 are shown in Table 1 and compared to literature values. The acyclic vinylethynyl radical ($H_2C{=}CH{-}C{\equiv}C^{\bullet}$) is found to be less stable, as are the cyclic radicals derived from cyclobutadiene (*cyclic*-C_4H_3) or *exo*-methylene cyclopropene (−C(CH)CHCH−).[32]

Calculated ionization energies (IE) for several C_4H_3 isomers are summarized in Table 2. An IE of 8.02 eV is obtained for *i*-C_4H_3, a value close to our observation, as shown in Figure 2. For *n*-C_4H_3, the results are rather complex. First, there are two forms for *n*-C_4H_3, the (*E*)-*n*- and the (*Z*)-*n*-C_4H_3. The ion state for the (*E*)-form optimizes to a ring with a vertical IE (9.77 eV) substantially larger than the adiabatic IE (8.25 eV), whereas the (*Z*)-form optimizes to the CH_2CCCH structure (*i*-form), again with a large difference between vertical (9.77 eV) and adiabatic (7.50 eV) ionization energies. The calculated vertical IE of *n*-C_4H_3 is marked in Figure 2 along with calculated adiabatic ionization energies to form triplet cations: 9.63 eV (*i*-$^3C_4H_3^+$), 9.71 eV [(*E*)-*n*-$^3C_4H_3^+$], and 9.70 eV [(*Z*)-*n*-$^3C_4H_3^+$]. Note that the adiabatic ionization energies calculated for the *cyclic*-C_4H_3 (7.20 eV) and the −C(CH)CHCH− isomers (7.35 eV) are too low to match the observed threshold near 8 eV. Furthermore, their high heats of formation relative to *i*-C_4H_3 suggest that they are unlikely to be present in high concentrations. The ionization energy for the CH_2CHCC isomer, which also has a high heat of formation, is calculated to be 9.91 eV, and no clear evidence for this isomer is observed.

C_4H_5. Selected structural C_4H_5 isomers have been the subject of previous quantum chemical studies.[35,37,38] The 1-methylallenyl (CH_3CCCH_2) isomer is found to be the lowest-energy point on the global C_4H_5 surface. The calculated enthalpies of formation for all $m/z = 53$ isomers considered in this paper are summarized in Table 3. The present calculations are in excellent agreement with earlier results published by Wheeler et al.[35] The second lowest-energy isomer is *i*-C_4H_5 (CH_2CHCCH_2), which is just

TABLE 1: Heats of Formation of Different C_4H_3 Isomers

species	$\Delta_fH°$ (0 K) (kcal mol^{-1}) HL[b]	literature[c]	Q1 diag.[a]
i-C_4H_3	119.1	119.0	0.021
(*E*)-*n*-C_4H_3	131.1	130.8	0.015
(*Z*)-*n*-C_4H_3	131.2	130.8	0.015
-C(CH)CHCH-	152.0		0.019
CH_2CHCC	153.9		0.023
cyclic-C_4H_3	155.4		0.026

[a] Q1 diagnostic. [b] Present higher-level calculated 0 K heat of formation in kcal mol^{-1}. [c] ref 35.

TABLE 2: Ionization Energies of Different C_4H_3 Isomers

species	ion state	ionization energies/eV calculated	measured	Q1 diag.[a]
i-C_4H_3	$^1A_1$	8.02	8.06 ± 0.05	0.025
	$^3A_2$	9.63		0.034
(*E*)-*n*-C_4H_3	$^1A_1$	9.77 (v)		0.030
		8.25 (a)		0.026
	$^3A''$	9.71		0.031
(*Z*)-*n*-C_4H_3	$^1A_1$	9.77 (v)		0.029
		7.50 (a)		0.034
	$^3A''$	9.70		0.031
-C(CH)CHCH-	$^1A'$	7.35		0.026
cyclic-C_4H_3	$^1A'$	7.20		0.026
CH_2CHCC	^1A	9.91		0.026

[a] Q1 diagnostic.

TABLE 3: Heats of Formation of Mass 53 Isomers

species	$\Delta_fH°$ (0 K) (kcal mol^{-1}) HL[b]	literature[c]	Q1 diag.[a]
CH_3CCCH_2	76.3		0.020
i-C_4H_5	78.7	78.4	0.023
CH_3CHCCH	79.1		0.020
cyclic-C_4H_5	80.4		0.011
(*E*)-*n*-C_4H_5	89.0	89.1	0.015
(*Z*)-*n*-C_4H_5	89.6	89.7	0.015
CH_2CH_2CCH	93.0		0.012
HCCCO	70.3		0.032

[a] Q1 diagnostic. [b] Present higher-level calculated 0 K heat of formation in kcal mol^{-1}. [c] ref 35.

TABLE 4: Ionization Energies of Mass 53 Isomers

species	ion state	ionization energies/eV calculated	literature[a]	measured	Q1 diag.[b]
CH_3CCCH_2	$^1A'$	7.94	7.95	7.97 ± 0.05	0.015
	^3A	9.74			0.026
i-C_4H_5	$^1A'$	7.55		7.60 ± 0.05	0.019
	$^3A''$	10.29			0.029
CH_3CHCCH	$^1A'$	7.95	7.97	7.97 ± 0.05	0.020
	^3A	10.20			0.030
cyclic-C_4H_5	$^1A'$	7.25			0.012
	$^3B_2$	9.99			0.023
(*E*)-*n*-C_4H_5	$^1A'$	7.10 (a)			0.019
		9.28 (v)			0.028
	$^3A''$	9.18			0.030
(*Z*)-*n*-C_4H_5	$^1A'$	7.08 (a)			0.019
		9.27 (v)			0.029
	$^3A''$	9.18			0.031
CH_2CH_2CCH	$^1A'$	7.50			0.011
HCCCO	$^1\Sigma_g$	7.36 (a)			0.020
		8.19 (v)			0.025

[a] ref 39. [b] Q1 diagnostic.

2.4 kcal mol^{-1} less stable than the most stable 1-methylallenyl. The often-considered *n*-C_4H_5 ($CH_2CHCHCH$) in its (*E*) and (*Z*) forms lies ~13 kcal mol^{-1} above the most stable CH_3CCCH_2. Because it is also possible that an $m/z = 53$ signal arises from C_3HO isomers, we also considered the HCCCO radical. Its calculated heat of formation is included in Table 3.

Calculated ionization energies for several C_4H_5 isomers and the HCCCO radical are summarized in Table 4. An IE of 7.55 eV is obtained for *i*-C_4H_5, a value close to the observed threshold, as shown in Figure 3. The second threshold in the PIE curve near 8.0 eV matches ionization energies of 7.94 and 7.95 eV, respectively, calculated for the CH_3CCCH_2 and CH_3-$CHCCH$ isomers, in good agreement with literature values.[39] The results are more complex for *n*-C_4H_5. Here again, there are two forms to consider: the (*E*)-*n*- and the (*Z*)-*n*-C_4H_5. The cations optimize to the CH_2CCCH structure (*i*-form), with a large difference between vertical (9.27 and 9.28 eV) and adiabatic (7.08 and 7.10 eV) ionization energies.

The ionization energy for the *cyclic*-C_4H_5 isomer (cyclobutadienyl radical) is calculated to be 7.25 eV, a value below the observed threshold. The calculated ionization energy of 7.50 eV for CH_2CH_2CCH is close to the observed threshold (Figure 3), and it could be formed easily by addition through $H + CH_2{=}CH{-}CCH$, but its high heat of formation relative to *i*-C_4H_5 argues against its prominence. For HCCCO, the situation is more complex. The $HCCCO^+$ ion is linear, compared to a bent structure in the radical ground state. The adiabatic and vertical ionization energies are calculated to be 7.36 and 8.19 eV, respectively, suggesting a small Franck−Condon overlap between the neutral and cation ground states. The simulation shows a gradual rise in photoionization efficiency throughout the 7.5−8.5 eV range, which does not match the observed structure.

4.2. Franck−Condon Modeling of the Photoionization Efficiency Spectra. The photoionization efficiency spectra of C_4H_3 and C_4H_5 are simulated using a calculated Franck−Condon envelope as a fitting function to estimate the adiabatic ionization energies of C_4H_3 and C_4H_5 isomers from the experimental data. A similar strategy was previously employed to derive the ionization energies of C_3H_2 (triplet propargylene) and HONO from flame measurements.[16,40] The simulations presented here are for an assumed temperature of 300 K. The temperatures in the sampled regions of the flames are considerably higher than 300 K, but significant cooling occurs in the expansion through the sampling nozzle. Rotational temperatures of NO sampled from similar flames have been measured to be between 300 and 400 K with little sensitivity to the initial sampling temperature.[41] In addition, photoionization efficiency curves of stable species, sampled at similar flame temperatures, agree well with room-temperature measurements.[14]

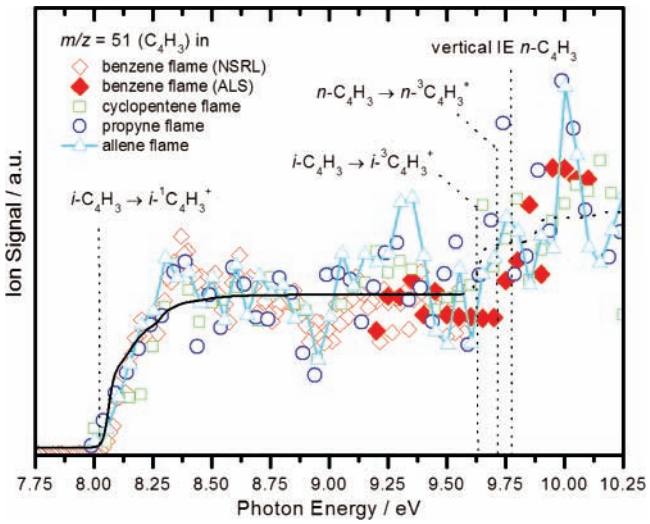

Figure 4. Comparison of the measured photoionization efficiency curve for $m/z = 51$ (C_4H_3) with a calculated Franck−Condon envelope for the *i*-C_4H_3 isomer (solid line). The observed threshold near 8 eV is the best fit with an IE of (8.06 ± 0.05) eV for the *i*-C_4H_3 isomer. No clear evidence for the *n*-C_4H_3 isomer is found. The dashed line indicates a Franck−Condon simulation for the *i*-$C_4H_3 \rightarrow$ *i*-$^3C_4H_3^+$ process.

C_4H_3. The *i*-C_4H_3 and the less stable *n*-C_4H_3 isomers are most likely to contribute to the $m/z = 51$ signal. The calculated IE of 8.02 eV for *i*-C_4H_3 closely matches the observed threshold. The simulated photoionization efficiency for *i*-C_4H_3 at 300 K is shown as a solid line in Figure 4, together with the observed PIE spectra. With the exception of the autoionization structure suggested by the data, the simulation follows the general trend of the PIE curve above threshold. An adiabatic ionization energy of 8.06 eV best reproduces the stepped increase at threshold. Systematic uncertainties are estimated to be ±0.05 eV, including ionization induced by the electric field between the repeller and extractor of the TOFMS, photon energy calibration error, and the use of the harmonic approximation in the Franck−Condon simulations. The adiabatic ionization energy of *i*-C_4H_3 is therefore reported as (8.06 ± 0.05) eV.

For *n*-C_4H_3, it is difficult to treat the transition from the neutral to the *cyclic*- or *i*-$C_4H_3^+$ cation accurately because of the difference between vertical and adiabatic ionization energies. A PIE that rises slowly above a poorly defined threshold might be expected for this situation, in contrast to the sharp step seen at threshold near 8.0 eV. However, the small increase in ion signal (i.e., in photoionization efficiency) for photon energies above 9.7 eV might be due to *n*-C_4H_3; the calculated IE to form *n*-$^3C_4H_3^+$ is 9.7 eV (cf. Table 2). On the other hand, this increase in the observed signal can also be taken as evidence for the formation of *i*-$^3C_4H_3^+$ ions. The simulated photoionization efficiency for the *i*-$C_4H_3 \rightarrow$ *i*-$^3C_4H_3^+$ process is shown in Figure 4 as a dashed line together with the already described curve for the formation of the singlet ion. The calculated ionization energy of 9.63 eV is used, and we note that both processes could describe the observed PIE curve.

C_4H_5. The *i*-C_4H_5 isomer can clearly be identified by its threshold in the PIE spectra near 7.6 eV. The calculated IE of 7.55 eV matches the observed threshold as shown in Figure 3. The simulated photoionization efficiency for *i*-C_4H_5 at 300 K

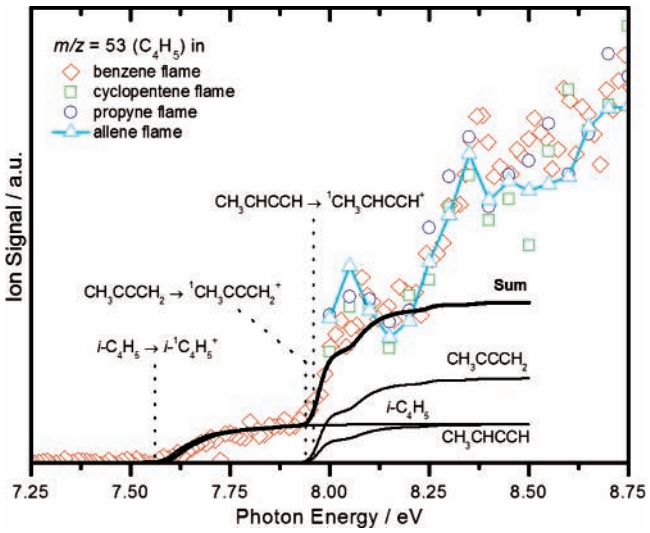

Figure 5. Simulated photoionization Franck−Condon envelopes for the *i*-C_4H_5 and the CH_3CCCH_2 and CH_3CHCCH isomers are compared with the experimental result. The observed photoionization efficiency curve below 8 eV can be explained by *i*-C_4H_5. Signal above 8 eV is most likely due to contributions of three different isomers: *i*-C_4H_5, CH_3CCCH_2 and CH_3CHCCH.

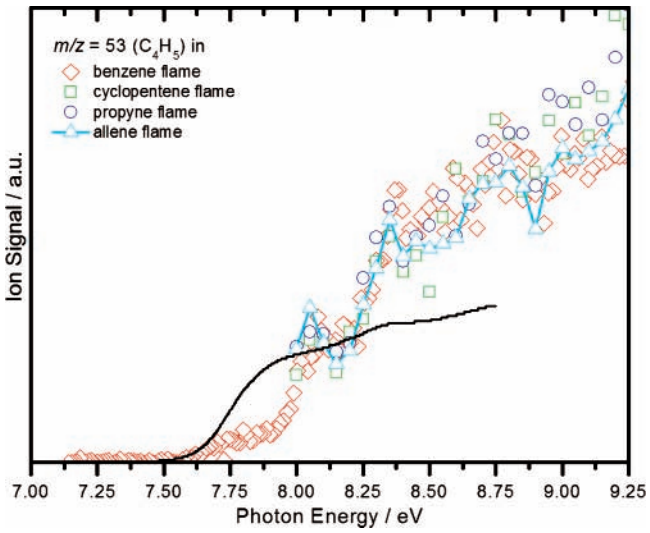

Figure 6. Simulated photoionization efficiency curve for the *cyclic*-C_4H_5 isomer based on the calculated ionization energy of 7.25 eV. The small ionization efficiency near the threshold is caused by a small Franck−Condon overlap between the neutral and the cation.

is shown in Figure 5, together with the observed PIE spectra. The simulation follows the observed curve perfectly above the threshold to a photon energy of ~8 eV. An adiabatic ionization energy of 7.60 eV best reproduces the observed curve. Again, systematic uncertainties are estimated to be ±0.05 eV, and therefore, we report the adiabatic ionization energy of *i*-C_4H_5 as (7.60 ± 0.05) eV. The threshold near 8.0 eV may arise from the CH_3CCCH_2 and CH_3CHCCH isomers, with calculated IEs in this region. Both isomers yield similar simulated PIE curves. Either isomer could be fit individually to the observed PIE spectra; however, because the heats of formation for these isomers are separated by just 2.8 kcal mol^{-1}, the presence of both isomers is expected, and therefore, the simulated PIE curve is a sum of contributions for both species. An ionization energy of 7.97 eV (for both species) best fits the data, which is in good agreement with calculated and measured IEs for CH_3CCCH_2 and CH_3CHCCH.[39]

In the best fit, the signal level from the CH_3CCCH_2 isomer at 8.25 eV is approximately twice the signal level of the *i*-C_4H_5 and CH_3CHCCH isomers. A direct determination of isomeric composition will require knowledge of the respective cross-sections for photoionization of each isomer. Assuming equal photoionization cross-sections for all three isomers, the observed concentrations are close to thermal equilibrium at the elevated temperatures in the low-pressure flames. At a typical flame temperature of 1700 K, one expects equilibrium ratios of CH_3CCCH_2/*i*-C_4H_5/CH_3CHCCH/*n*-C_4H_5 = 1/0.49/0.44/0.02.

The increase of the photoionization efficiency above 8.2 eV shown in Figures 3 and 5 cannot be explained by our current model. This may be partially attributable to limitations of the harmonic approximation, which become more important for photon energies well above the threshold. The formation of excited triplet states of the ions can be ruled out, as our calculations indicate (Table 4) that those states do not contribute at photon energies below 9.74 eV. At thermal equilibrium, one would expect a considerable amount of *cyclic*-C_4H_5, but the Franck−Condon overlap between the ground-state neutral and the cation is small. The simulations for *cyclic*-C_4H_5 show a PIE curve rising slowly above the calculated ionization energy as shown in Figure 6. The *n*-C_4H_5 radical is not a likely candidate to explain the increase in photoionization efficiency. First, because of its thermodynamic instability compared to CH_3CCCH_2, it is less likely to be present in high concentrations. Second, the poor Franck−Condon overlap between the neutral and the ion makes it hard to detect by photoionization mass spectrometry. Franck−Condon simulations were performed for the HCCCO radical, but they also failed to explain the PIE curve above 8.25 eV.

4.3. Literature Flame Data and Combustion Chemistry. Both C_4H_3 and C_4H_5 have been observed previously in numerous flames, but their identities have been uncertain.[3,42−53] Previous flame sampling molecular beam mass spectrometry measurements of C_4H_3 and C_4H_5, using electron ionization, are summarized in Table 5. Measurements are only included when appearance energies were determined. Estimating cross-sections for electron ionization requires knowledge of the ionization energies; the apparent ionization thresholds used to determine the mole fractions in the literature experiments are also given in Table 5. The apparent ionization thresholds in the electron ionization experiments are typically determined by linear extrapolation of the observed ion signals down to the baseline, and naturally depend on the electron energy resolution and the signal-to-noise ratio. In most cases, the apparent thresholds do not suffice for determining isomeric composition. Nevertheless, comparison of the present photoionization measurements with the lower-resolution electron ionization measurements can highlight common broad features of the ionization efficiency spectra.

C_4H_3. The first measurement of C_4H_3 was in a $\phi = 2.4$ C_2H_2 flame by Westmoreland. It displayed an apparent ionization threshold of (8.6 ± 0.7) eV by electron ionization,[42,54] which this work shows to be consistent with *i*-C_4H_3. Analysis of the acetylene flame showed that the reactions $C_4H_3 + C_2H_2 \rightarrow$ phenyl and/or $C_4H_5 + C_2H_2 \rightarrow$ benzene + H and/or $2C_3H_3 \rightarrow$ products could potentially account for all of the rate of mass 78 formation, where the C_4H_3 and C_4H_5 isomers were left unidentified.[3]

For C_4H_3, other electron-ionization measurements show apparent thresholds near 9.4 eV, which are substantially higher than the *i*-C_4H_3 ionization energy. The further exception was the fuel-rich benzene flame of Bittner,[52] where an apparent threshold of (10.3 ± 0.3) eV was reported. The only C_4H_3

TABLE 5: Previous Flame Measurements of C_4H_3 and C_4H_5 Using Electron-Ionization Molecular Beam Mass Spectrometry

	$m/z = 51$ (C_4H_3)					$m/z = 53$ (C_4H_5)					
flame	apparent threshold (eV)	meas. at z (mm)	max mole fraction	meas. at z (mm)	meas. at (eV)	apparent threshold (eV)	meas. at z (mm)	max mole fraction	meas. at z (mm)	meas. at (eV)	refs
C_2H_2 $\phi = 2.4$, 5.0% Ar	8.6 ± 0.7		$2 \cdot 10^{-5}$	4.3	10.85	8.9 ± 0.3	3.2	$1.0 \cdot 10^{-5}$	2.2	10.85	3, 42
C_2H_4, $\phi = 1.9$, 5.0% Ar	9.5 ± 0.5	8.0	$6.7 \cdot 10^{-6}$	8.1	11.25	not measured		$2.9 \cdot 10^{-6}$	6.8	11.25	44, 45
allene-doped C_2H_4 $\phi = 1.9$, 5.0% Ar	9.3 ± 0.4	8.0	$1.3 \cdot 10^{-4}$	9.3	11.76	9.0 ± 0.4	6.0	$2.4 \cdot 10^{-5}$	7.1	11.76	46
propene $\phi = 1.64$, 6.71% Ar	9.4 ± 0.4	5.8	$5 \cdot 10^{-5}$	2.8	10.66	9.1 ± 0.4	4.6	$2 \cdot 10^{-5}$	4	10.66	47, 53
1,3-butadiene $\phi = 1.0$, 60% Ar	not measured		$4 \cdot 10^{-6}$	4.6		7.7 ± 0.4		$2.8 \cdot 10^{-5}$	3.3		49
benzene $\phi = 1.8$, 30% Ar	10.3 ± 0.3	6.6	$2 \cdot 10^{-4}$	8.4	10.3	9.4 ± 0.3	7.0	$3 \cdot 10^{-5}$	6.8	10.3	52

species with an ionization energy in that region is the carbene, CH_2CHCC, which is unlikely to be present in substantial concentrations, based on thermochemical considerations. It appears likely that he picked up the signal from a ^{13}C isotopomer of diacetylene (IP = 10.17 eV).

In the present work, the *i*-C_4H_3 isomer has been specifically identified as present in fuel-rich allene, propyne, cyclopentene, and benzene flames. Assuming that the $m/z = 51$ signal at 10 or 9.8 eV is due solely to *i*-C_4H_3, the peak mole fraction is 1.6×10^{-5} in the cyclopentene flame and 8×10^{-5} in the fuel-rich allene flame. In hydrocarbon combustion processes, both the *i*- and the *n*-C_4H_3 isomers can be produced by H addition to butadiyne and by H abstraction from vinylacetylene ($CH_2{=}CH{-}C{\equiv}CH$). Perhaps because of the large differences between vertical and adiabatic ionization energies for the *n*-C_4H_3 isomer, no clear evidence for *n*-C_4H_3 is found in this work. Nevertheless, if the small increase in photoionization efficiency above 9.7 eV should be caused by *n*-C_4H_3 being ionized to form triplet *n*-$C_4H_3^+$, an upper bound for the *n*-C_4H_3 mole fraction can be estimated. Assuming equal photoionization cross-sections to the triplet ion for *i*- and *n*-C_4H_3 near 10 eV, about 20% of the signal would be due to *n*-C_4H_3 and 60% of the signal would be due to the *i*-$C_4H_3 \rightarrow$ *i*-$^1C_4H_3^+$ process, while another 20% is due to the formation of *i*-$^3C_4H_3^+$. The peak mole fractions for *n*-C_4H_3 would be estimated to be below 3×10^{-6} and 1×10^{-5} in the cyclopentene and allene flames, respectively. This upper bound on the *n*-C_4H_3/*i*-C_4H_3 ratio is substantially higher than the expected ratio at thermal equilibrium ($\sim$0.03 at 1700 K) but may still be low enough to rule out *n*-C_4H_3 as a *principal* precursor to benzene formation for the flames considered here. The upper bound could be substantially higher if more of the steps were due to this species, i.e., if the photoionization cross-section were smaller.

The estimated mole fractions for *i*-C_4H_3 and the upper bounds for *n*-C_4H_3 should be valuable in detailed modeling studies of the possible importance of the $C_4H_3 + C_2H_2$ reactions as important benzene formation pathways. In particular, the reaction of *i*-C_4H_3 plus acetylene deserves testing in chemical kinetics models. Walch[11] and Klippenstein and Miller[13] have shown that this reaction can also yield the phenyl radical (or *o*-benzyne + H) by a pathway that involves no barriers that lie higher in energy than the entrance-channel addition barrier. Recent electronic-structure calculations indicate that the barrier for *i*-C_4H_3 addition to acetylene is smaller than previously thought.[13]

The participation of the *i*- and *n*-C_4H_3 isomers in cyclization steps must be weighed against thermal dissociation and hydrogen abstraction reactions, which may occur rapidly in the high-temperature reaction zones of premixed flames. In fact, *i*- and *n*-C_4H_3 isomers share a property with many small unsaturated, even resonantly stabilized, free hydrocarbon radicals: They have relatively weak C−H bonds (important exceptions are isomers of C_3H_2, C_3H_3, and C_5H_3). This property is a result of the fact that these radicals can dissociate into a stable molecule and a hydrogen atom, as opposed to two radicals. This elusive chemistry makes accurate, reliable measurements of their concentrations extremely important.

C_4H_5. There are at least five isomers of C_4H_5 that could be detectable in the flames studied experimentally in this paper: *cyclic*-C_4H_5, *n*-C_4H_5 ($CH_2CHCHCH$), *i*-C_4H_5 (CH_2CCHCH_2), 1-methylallenyl (CH_3CCCH_2), and a CH_3CHCCH isomer. The least significant of these is probably *cyclic*-C_4H_5. It can be formed either as a minor product at low or intermediate temperatures in the reaction of vinyl with acetylene or from the direct isomerization, *n*-$C_4H_5 \rightarrow$ *cyclic*-C_4H_5.[38,55] At temperatures typical of the reaction zones of premixed flames, the equilibrium of this isomerization shifts to favor *n*-C_4H_5, making *cyclic*-C_4H_5 unstable with respect to isomerization. Consequently, the presence of *cyclic*-C_4H_5 in flames should be limited to the low-temperature regions. The cooling process that occurs during the sampling may lead to the quenching of some of the more highly excited *n*-C_4H_5 into the cyclic species; however, that does not appear to be the case, since no evidence for *cyclic*-C_4H_5 is found.

Probably because of the large differences between vertical and adiabatic ionization energies, no clear evidence is found for the *n*-C_4H_5 isomer in the present work. In previous work, using electron ionization, appearance energies near 9 eV were measured, except Cole who measured an apparent ionization energy of (7.7 ± 0.4) eV in a stoichiometric 1,3-butadiene flame.[49] Bittner measured an ionization threshold of (9.4 ± 0.3) eV,[52,56] and subsequently, Westmoreland measured an ionization threshold of (8.9 ± 0.25) eV in a fuel-rich C_2H_2 flame.[42] These values are consistent with ionization of *n*-C_4H_5 to a triplet state (Table 4), but no threshold was reported at the ionization energy to the singlet ion, 7.1 eV.

Thermochemistry and much formation chemistry favor *i*-C_4H_5. In high-temperature reaction zones of rich flames, *n*-C_4H_5 can be easily converted to the more stable *i*-isomer by H-atom-assisted isomerization.[4] *i*-C_4H_5 should also be the dominant abstraction product of 1,3-butadiene + radical reactions because of the weaker allylic H at the 2-position compared to the vinylic H at the 1-position. This hypothesis is supported by the

ionization threshold for C_4H_5 [(7.7 ± 0.4) eV] measured by Cole[57] in a stoichiometric 1,3-butadiene flame.

The overall reaction n-$C_4H_5 + C_2H_2 \rightarrow$ benzene + H was proposed as an important cyclization step under combustion conditions by Cole et al.,[57] Weissman and Benson,[58,59] Frenklach and co-workers,[60,61] and Westmoreland et al.[3] This role for n-C_4H_5 was given credence in the experiments of Callear and Smith,[62,63] who were studying the reaction of H with acetylene at low temperature and discovered large quantities of benzene in the products. They proposed that the n-C_4H_5 came from the sequence

$$H + C_2H_2 (+ M) \rightarrow C_2H_3 (+ M)$$

$$C_2H_3 + C_2H_2 (+ M) \rightarrow n\text{-}C_4H_5 (+ M)$$

Miller et al.[38] have shown theoretically that indeed n-C_4H_5 is the dominant product of the $C_2H_3 + C_2H_2$ reaction at low temperatures, and the above sequence remains a possible source of benzene in the low-temperature regions of premixed flames.

Miller and Melius[4] suggested that the reaction of i-C_4H_5 with acetylene was a plausible cyclization step under certain flame conditions. This reaction can form fulvene + H without undergoing any H-atom transfers or going through any multicentered transition states after the initial complex is formed.[4,64−66] It deserves more consideration than it has been given to date.

1-Methylallenyl is formed in flames primarily from the reaction of methyl with propargyl.[64−67] As it is simply a methyl-substituted propargyl radical, it can react with propargyl to form toluene or benzyl + H through a sequence of steps analogous to those by which the propargyl + propargyl reaction forms benzene and phenyl + H.[8] Similarly, 1-methylallenyl can react with itself, leading ultimately to *ortho*-xylene. The CH_3CHCCH isomer is also a methyl-substituted propargyl radical that can be formed from the $CH_3 + C_3H_3$ reaction. It is only slightly less stable thermodynamically than i-C_4H_5 and 1-methylallenyl. Although it appears currently to be absent from flame models, it conceivably could play a role in the cyclization and precyclization chemistry. The role of all different C_4H_5 isomers in cyclization reactions requires further investigation.

5. Conclusions

C_4H_3 and C_4H_5 isomers in fuel-rich allene, propyne, cyclopentene, and benzene flames are identified by combining photoionization mass spectrometry using tunable vacuum-ultraviolet synchrotron radiation with ab initio-based Franck−Condon simulations. On the basis of calculated frequencies and force constants, the Franck−Condon analysis suggests that mostly i-C_4H_3 is detected at $m/z = 51$ and that i-C_4H_5, CH_3-$CCCH_2$, and/or CH_3CHCCH isomers are present at $m/z = 53$. The small amount of n-C_4H_3 together with large differences in vertical and adiabatic ionization energies may make it difficult to detect n-C_4H_3. However, the reaction of i-C_4H_3 with acetylene to form phenyl or *o*-benzyne should be considered as a possible cyclization step. The detection of i-C_4H_5 suggests that its reaction with acetylene to form fulvene + H is a plausible cyclization step. The role in soot formation of 1-methylallenyl (CH_3CCCH_2) and/or the CH_3CHCCH isomer, which is currently absent from flame models, requires further investigation. Because of low Franck−Condon factors, sensitivity to the less stable n-C_4H_5 is limited, and no clear evidence for this isomer was found in the present flames. The data allowed determination of the ionization energies of i-C_4H_3 [(8.06 ± 0.05) eV], of i-C_4H_5 [(7.60 ± 0.05) eV], and (7.97 ± 0.05) eV for either CH_3CCCH_2 and/or CH_3CHCCH.

Acknowledgment. The authors gratefully acknowledge Dr. Paul Winter, Prof. Timothy Zwier, and Jaime Stearns for supplying the computer program used to evaluate the Franck−Condon factors and for assistance in its use. Tina Kasper and Katharina Kohse-Höinghaus (Universität Bielefeld, Germany) suggested the study of cyclopentene flames and provided helpful discussions on cyclopentene flame modeling. We thank Patrick Osswald (Universität Bielefeld) for his help resolving a discrepancy between the NSRL and ALS experiments. The authors are grateful to Paul Fugazzi for expert technical assistance. This work is supported by the Division of Chemical Sciences, Geosciences, and Biosciences, the Office of Basic Energy Sciences, the U. S. Department of Energy, in part under grants DE-FG02-91ER14192 (P.R.W., M.E.L.) and DE-FG02-01ER-15180 (T.A.C., J.W.), and by the Chemical Science Division of the U. S. Army Research Office. F.Q. is supported by the Chinese Academy of Sciences under grant no. 1731230600001 and the National Natural Science Foundation of China under grant no. 20473081. Sandia is a multiprogram laboratory operated by Sandia Corporation, a Lockheed Martin Company, for the National Nuclear Security Administration under contract DE-AC04-94-AL85000. The Advanced Light Source is supported by the Director, Office of Science, Office of Basic Energy Sciences, Materials Sciences Division, of the U. S. Department of Energy under contract no. DE-AC02-05C.H.11231 at Lawrence Berkeley National Laboratory. Ford Motor Company is gratefully acknowledged for supplying the propyne used in some of these experiments.

References and Notes

(1) Denissenko, M. F.; Pao, A.; Tang, M. S.; Pfeifer, G. P. *Science* **1996**, *274*, 430.
(2) Durant, J. L.; Busby, W. F.; Lafleur, A. L.; Penman, B. W.; Crespi, C. L. *Mutat. Res.* **1996**, *371*, 123.
(3) Westmoreland, P. R.; Dean, A. M.; Howard, J. B.; Longwell, J. P. *J. Phys. Chem.* **1989**, *93*, 8171.
(4) Miller, J. A.; Melius, C. F. *Combust. Flame* **1992**, *91*, 21.
(5) Pope, C. J.; Miller, J. A. *Proc. Combust. Inst.* **2000**, *28*, 1519.
(6) Frenklach, M. *Phys. Chem. Chem. Phys.* **2002**, *4*, 2028.
(7) Richter, H.; Howard, J. B. *Phys. Chem. Chem. Phys.* **2002**, *4*, 2038.
(8) Miller, J. A.; Klippenstein, S. J. *J. Phys. Chem. A* **2003**, *107*, 7783.
(9) Kohse-Höinghaus, K.; Atakan, B.; Lamprecht, A.; Alatorre, G. G.; Kamphus, M.; Kasper, T.; Liu, N. N. *Phys. Chem. Chem. Phys.* **2002**, *4*, 2056.
(10) Atakan, B.; Lamprecht, A.; Kohse-Höinghaus, K. *Combust. Flame* **2003**, *133*, 431.
(11) Walch, S. P. *J. Chem. Phys.* **1995**, *103*, 8544.
(12) Klippenstein, S. J.; Miller, J. A. *J. Phys. Chem. A* **2005**, *109*, 4285.
(13) Klippenstein, S. J.; Miller, J. A. Unpublished.
(14) Cool, T. A.; Nakajima, K.; Mostefaoui, T. A.; Qi, F.; McIlroy, A.; Westmoreland, P. R.; Law, M. E.; Poisson, L.; Peterka, D. S.; Ahmed, M. *J. Chem. Phys.* **2003**, *119*, 8356.
(15) Taatjes, C. A.; Hansen, N.; McIlroy, A.; Miller, J. A.; Senosiain, J. P.; Klippenstein, S. J.; Qi, F.; Sheng, L.; Zhang, Y.; Cool, T. A.; Wang, J.; Westmoreland, P. R.; Law, M. E.; Kasper, T.; Kohse-Höinghaus, K. *Science* **2005**, *308*, 1887.
(16) Taatjes, C. A.; Klippenstein, S. J.; Hansen, N.; Miller, J. A.; Cool, T. A.; Wang, J.; Law, M. E.; Westmoreland, P. R. *Phys. Chem. Chem. Phys.* **2005**, *7*, 806.
(17) Cool, T. A.; McIlroy, A.; Qi, F.; Westmoreland, P. R.; Poisson, L.; Peterka, D. S.; Ahmed, M. *Rev. Sci. Instrum.* **2005**, *76*, 094102.
(18) Tanaka, K.; Tanaka, I. *J. Chem. Phys.* **1973**, *59*, 5042.
(19) Nicholson, A. J. C. *J. Chem. Phys.* **1963**, *39*, 954.
(20) Melius, C. F.; Colvin, M. E.; Marinov, N. M.; Pitz, W. J.; Senkan, S. M. *Proc. Combust. Inst.* **1996**, *26*, 685.
(21) Cool, T. A.; Nakajima, K.; Taatjes, C. A.; McIlroy, A.; Westmoreland, P. R.; Law, M. E.; Morel, A. *Proc. Combust. Inst.* **2005**, *30*, 1681.
(22) Robinson, J. C.; Sveum, N. E.; Neumark, D. M. *J. Chem. Phys.* **2003**, *119*, 5311.

(23) Robinson, J. C.; Sveum, N. E.; Neumark, D. M. *Chem. Phys. Lett.* **2004**, *383*, 601.
(24) Becke, A. D. *J. Chem. Phys.* **1993**, *98*, 5648.
(25) Hehre, W. J.; Radom, L.; Pople, J. A.; Schleyer, P. v. R. *Ab Initio Molecular Orbital Theory*; Wiley: New York, 1987.
(26) Frisch, M. J.; Trucks, G. W.; Schlegel, H. B.; Scuseria, G. E.; Robb, M. A.; Cheeseman, J. R.; Montgomery Jr., J. A.; Vreven, T.; Kudin, K. N.; Burant, J. C.; Millam, J. M.; Iyengar, S. S.; Tomasi, J.; Barone, V.; Mnnucci, B.; Cossi, M.; Scalmani, G.; Rega, N.; Petersson, G. A.; Nakatsuji, H.; Hada, M.; Ehara, M.; Toyota, K.; Fukuda, R.; Hasegawa, J.; Ishida, M.; Nakajima, T.; Honda, O.; Kitao, H.; Nakai, H.; Klene, M.; Li, X.; Knox, J. E.; Hratchian, H. P.; Cross, J. B.; Bakken, V.; Adamo, C.; Jaramillo, J.; Gomperts, R.; Stratmann, R. E.; Yazyev, O.; Austin, A. J.; Cammi, R.; Pomelli, C.; Ochterski, J. W.; Ayala, P. Y.; Morokuma, K.; Voth, G. A.; Salvador, P.; Dannenberg, J. J.; Zakrzewski, V. G.; Dapprich, S.; Daniels, A. D.; Strain, M. C.; Farkas, O.; Malick, D. K.; Rabuck, A. D.; Raghavachari, K.; Foresman, J. B.; Ortiz, J. V.; Cui, Q.; Baboul, A. G.; Clifford, S.; Cioslowski, J.; Stefanov, B. B.; Liu, G.; Liashenko, A.; Piskorz, P.; Komaromi, I.; Martin, R. L.; Fox, D. J.; Keith, T.; Al-Laham, M. A.; Peng, C. Y.; Nanayakkara, A.; Challacombe, M.; Gill, P. M. W.; Johnson, B.; Chen, W.; Wong, M. W.; Gonzalez, C.; Pople, J. A. *Gaussian 03*, revision C.02; Gaussian, Inc.: Wallingford, CT, 2004.
(27) Dunning, T. H. *J. Chem. Phys.* **1989**, *90*, 1007.
(28) Amos, R. D.; Bernhardsson, A.; Berning, A.; Celani, P.; Cooper, D. L.; Deegan, M. J. O.; Dobbyn, A. J.; Eckert, F.; Hampel, C.; Hetzer, G.; Knowles, P. J.; Korona, T.; Lindh, R.; Lloyd, A. W.; McNicholas, S. J.; Manby, F. R.; Meyer, W.; Mura, M. E.; Nicklass, A.; Palmieri, P.; Pitzer, R.; Rauhut, G.; Schutz, M.; Schumann, U.; Stoll, H.; Stone, A. J.; Tarroni, R.; Thorsteinsson, T.; Werner, H.-J. MOLPRO, a package of ab initio programs designed by H.-J. Werner and P. J. Knowles, 2002.
(29) Doktorov, E. V.; Malkin, I. A.; Man'ko, V. I. *J. Mol. Spectrosc.* **1977**, *64*, 302.
(30) Ruhoff, P. T. *Chem. Phys.* **1994**, *186*, 355.
(31) Ramos, C.; Winter, P. R.; Zwier, T. S.; Pratt, S. T. *J. Chem. Phys.* **2002**, *116*, 4011.
(32) Ha, T.-K.; Gey, E. *THEOCHEM* **1994**, *306*, 197.
(33) Cioslowski, J.; Liu, G. H.; Moncrieff, D. *J. Phys. Chem. A* **1999**, *103*, 11465.
(34) Le, T. N.; Mebel, A. M.; Kaiser, R. I. *J. Comput. Chem.* **2001**, *22*, 1522.
(35) Wheeler, S. E.; Allen, W. D.; Schaefer, H. F. *J. Chem. Phys.* **2004**, *121*, 8800.
(36) Krokidis, X.; Moriarty, N. W.; Lester, W. A.; Frenklach, M. *Int. J. Chem. Kinet.* **2001**, *33*, 808.
(37) Wang, H.; Frenklach, M. *J. Phys. Chem.* **1994**, *98*, 11465.
(38) Miller, J. A.; Klippenstein, S. J.; Robertson, S. H. *J. Phys. Chem. A* **2000**, *104*, 7525 and 9806 (Correction).
(39) Lias, S. G.; Bartmess, J. E.; Liebman, J. F.; Holmes, J. L.; Levin, R. D.; Mallard, W. G. *J. Phys. Chem. Ref. Data* **1988**, *17*, 1.
(40) Taatjes, C. A.; Osborn, D. L.; Cool, T. A.; Nakajima, K. *Chem. Phys. Lett.* **2004**, *394*, 19.
(41) Kamphus, M.; Liu, N. N.; Atakan, B.; Qi, F.; McIlroy, A. *Proc. Combust. Inst.* **2003**, *29*, 2627.
(42) Westmoreland, P. R. Experimental and Theoretical Analysis of Oxidation and Growth Chemistry in a Fuel-Rich Acetylene Flame. Ph.D. Dissertation, Massachusetts Institute of Technology, 1986.
(43) Lamprecht, A.; Atakan, B.; Kohse-Höinghaus, K. *Combust. Flame* **2000**, *122*, 483.
(44) Bhargava, A. A Molecular-Beam Mass Spectrometry Study and Modeling of Ethylene Flames. Ph.D. Dissertation, University of Massachusetts, Amherst, 1997.
(45) Bhargava, A.; Westmoreland, P. R. *Combust. Flame* **1998**, *113*, 333.
(46) Oulundsen, G. E. Measurements and Kinetics for Hydrocarbon−Chlorine and Allene-Doped Ethylene Flames. Ph.D. Dissertation, University of Massachusetts, Amherst, 1999.
(47) Thomas, S. D. Molecular-Beam Mass Spectrometry and Mechanistic Modeling of Lean and Rich Propene Flames. Ph.D. Dissertation, University of Massachusetts, Amherst, 1992.
(48) Morel, A. Molecular-Beam Mass Spectrometer Measurements and Modeling of Propene and Related Flames. M.S. Thesis, University of Massachusetts, Amherst, 2005.
(49) Cole, J. A. A Molecular-Beam Mass Spectrometric Study of Stoichiometric and Fuel-Rich 1,3-Butadiene Flames. M.S. Thesis, Massachusetts Institute of Technology, 1982.
(50) Lamprecht, A.; Atakan, B.; Kohse-Höinghaus, K. *Proc. Combust. Inst.* **2000**, *28*, 1817.
(51) Alatorre, G. G.; Böhm, H.; Atakan, B.; Kohse-Höinghaus, K. *Z. Phys. Chem.* **2001**, *218*, 981.
(52) Bittner, J. D. A Molecular Beam Mass Spectrometer Study of Fuel-Rich and Sooting Benzene-Oxygen Flames. Ph.D. Dissertation, Massachusetts Institute of Technology, 1981.
(53) Thomas, S. D.; Bhargava, A.; Westmoreland, P. R.; Lindstedt, R. P.; Skevis, G. *Bull. Soc. Chim. Belg.* **1996**, *105*, 501.
(54) Westmoreland, P. R.; Howard, J. B.; Longwell, J. P. *Proc. Combust. Inst.* **1986**, *21*, 773.
(55) Klippenstein, S. J.; Miller, J. A. *J. Phys. Chem. A* **2002**, *106*, 9267.
(56) Bittner, J. D.; Howard, J. B. *Proc. Combust. Inst.* **1981**, *18*, 1105.
(57) Cole, J. A.; Bittner, J. D.; Longwell, J. P.; Howard, J. B. *Combust. Flame* **1984**, *56*, 51.
(58) Weissman, M.; Benson, S. W. *Int. J. Chem. Kinet.* **1984**, *16*, 307.
(59) Weissman, M.; Benson, S. W. *Prog. Energy Combust. Sci.* **1989**, *15*, 273.
(60) Frenklach, M.; Clary, D. W.; Gardiner, W. C.; Stein, S. E. *Proc. Combust. Inst.* **1985**, *20*, 887.
(61) Frenklach, M.; Warnatz, J. *Combust. Sci. Technol.* **1987**, *51*, 265.
(62) Callear, A. B.; Smith, G. B. *Chem. Phys. Lett.* **1984**, *105*, 119.
(63) Callear, A. B.; Smith, G. B. *J. Phys. Chem.* **1986**, *90*, 3229.
(64) Miller, J. A.; Pilling, M. J.; Troe, J. *Proc. Combust. Inst.* **2005**, *30*, 43.
(65) Miller, J. A. *Proc. Combust. Inst.* **1996**, *26*, 461.
(66) Miller, J. A. *Faraday Discuss.* **2001**, *119*, 461.
(67) Marinov, N. M.; Pitz, W. J.; Westbrook, C. K.; Castaldi, M. J.; Senkan, S. M. *Combust. Sci. Technol.* **1996**, *116*, 211.